

SCIENTIFIC REPORTS

OPEN

Frataxin overexpression in Müller cells protects retinal ganglion cells in a mouse model of ischemia/reperfusion injury *in vivo*

Rowena Schultz¹, Melanie Krug², Michel Precht², Stefanie G. Wohl³, Otto W. Witte² & Christian Schmeer²

Müller cells are critical for retinal function and neuronal survival but can become detrimental in response to retinal ischemia and increased oxidative stress. Elevated oxidative stress increases expression of the mitochondrial enzyme frataxin in the retina, and its overexpression is neuroprotective after ischemia. Whether frataxin expression in Müller cells might improve their function and protect neurons after ischemia is unknown. The aim of this study was to evaluate the effect of frataxin overexpression in Müller cells on neuronal survival after retinal ischemia/reperfusion in the mouse *in vivo*. Retinal ischemia/reperfusion was induced in mice overexpressing frataxin in Müller cells by transient elevation of intraocular pressure. Retinal ganglion cells survival was determined 14 days after lesion. Expression of frataxin, antioxidant enzymes, growth factors and inflammation markers was determined with qRT-PCR, Western blotting and immunohistochemistry 24 hours after lesion. Following lesion, there was a 65% increase in the number of surviving RGCs in frataxin overexpressing mice. Improved survival was associated with increased expression of the antioxidant enzymes *Gpx1* and *Sod1* as well as the growth factors *Cntf* and *Lif*. Additionally, microglial activation was decreased in these mice. Therefore, support of Müller cell function constitutes a feasible approach to reduce neuronal degeneration after ischemia.

One key element of the pathologic alteration in retinal ischemia/reperfusion injury is the generation of excessive reactive oxygen species (ROS) during reperfusion. Retinal glia (i.e., Müller cells and astrocytes) play a fundamental role in maintaining redox homeostasis and are equipped with tools to resolve redox imbalance^{1,2}. Müller cells (MG) are the predominant glia in the vertebrate retina, expand the entire retina forming a structural scaffolding and have cell contacts to all neuronal cell types in the different retinal layers. Therefore they can form a functional unit with a more critical role than for astrocytes, which are restricted to the nerve fiber layer¹. After injury, Müller cells become reactive and participate in glial scar formation. Interestingly, metabolic support of neurons by Müller cells has been shown to be compatible, even with proliferative reactive gliosis induced in mice³. However, morphological and functional alterations in the MG have been found under ischemic conditions or elevated levels of oxidative stress⁴, which probably compromise their supportive role.

Mitochondria are the main source of free radical production in the cell, under both, normal and ischemic conditions^{5,6}. Following ischemic injury, endogenous mechanisms of cellular defense are activated to minimize damage. These include superoxide dismutases (SODs), glutathione, vitamins A, C, and E, catalase and other peroxidases. Moreover, recent evidence supports a role for the mitochondrial protein frataxin (FXN) in various diseases, which are caused by increased oxidative stress. FXN deficiency is closely associated with increased oxidative stress damage in Friedreich ataxia (FRDA), an autosomal recessive disease characterized by progressive neurodegeneration in the spinal cord and hypertrophic cardiomyopathy⁷⁻⁹. FXN acts as an important regulator of mitochondrial energy metabolism^{10,11} and is involved in several important functions including cellular iron homeostasis and redox balance during oxidative stress⁷. The mature FXN protein is highly expressed in mitochondria of metabolically active tissues such as liver, skeletal and cardiac muscle, and brain¹². In the adult mouse

¹Department of Ophthalmology, Jena University Hospital, Jena, Germany. ²Hans-Berger Department of Neurology, Jena University Hospital, Jena, Germany. ³Department of Biological Structure, University of Washington Seattle, Seattle, United States. Correspondence and requests for materials should be addressed to C.S. (email: christian.schmeer@med.uni-jena.de)

retina, immunoreactivity to FXN has been shown in the outer and inner plexiform layers, the ganglion cell layer and the inner nuclear layer. Highest levels of FXN were observed in inner segments of the photoreceptor cells¹³.

Improving essential functions of glia was shown to augment glial support to retinal neurons¹. In particular, support of the glial management of retinal redox homeostasis has been proposed as a therapeutic alternative to overcome neuronal degeneration due to excessive oxidative stress¹. Because Müller cells span the entire retina and quickly respond to injury, they are ideal targets for therapeutic strategies, including gene therapy¹⁴. Delivery of exogenous antioxidants or the manipulation of antioxidant pathways within the retina favors the interaction between retinal glia and neurons, and improves RGC survival and function^{1,15}. In particular, FXN overexpression was found to stimulate the production of ATP and to induce the activation of antioxidant mechanisms⁸. In a previous study, we found an increased expression of endogenous FXN in the mouse retina 24 hours after an ischemic lesion, indicating that FXN is involved in neuroprotective mechanisms in response to ischemic retinal injury¹⁶. Furthermore, in the same study, we showed that ubiquitous overexpression of human FXN under the transcriptional control of a human cytomegalovirus (CMV) minimal promoter resulted in neuronal protection. Neuroprotection was associated with changes in expression levels of some stress response molecules, including *Hmox1* and *Hif-2 α* , which suggested the participation of glial cells, particularly Müller cells, in FXN-mediated neuroprotection. To further evaluate the cellular mechanisms involved in the FXN-mediated neuroprotection in the ischemic retina and the putative role of Müller cells, here we used a conditional transgenic mouse model overexpressing the human FXN gene specifically in these cells.

Results

FXN expression was increased in the retina of naïve MGCRe-FXN mice and specifically localized to Müller cells. To evaluate the effect of FXN overexpression in Müller cells on neuronal survival after ischemia, we generated transgenic mice specifically expressing the human FXN cDNA and EGFP transcript in Müller cells (referred to as MGCRe-FXN mice, see materials and methods).

Quantification of mRNA for both, murine and human FXN, showed specific expression of the human FXN transcript in the retina of FXN overexpressing mice (Fig. 1A) and increased levels for endogenous mouse FXN compared with MGCRe-B6 mice (1.00 ± 0.05 vs. 1.50 ± 0.11 -fold increase, $P < 0.001$). The Western blot analysis showed higher levels of expression for both, precursor (30 kDa) and mature FXN protein (18 kDa) in MGCRe-FXN mice, compared to MGCRe-B6 mice (45% and 65% increase respectively, $P < 0.05$, Fig. 1B). However, human FXN protein was indistinguishable from the endogenous mouse variant (Fig. 1B').

To prove the cellular localization of human FXN, retinal slices were co-stained with anti-GFP and the Müller cell-specific marker glutamine synthetase (GS). EGFP was specifically localized in cells spanning the whole retina from FXN overexpressing mice (Fig. 1C). The expression of EGFP was co-localized with the specific Müller cells marker GS in the retina from the MGCRe-FXN mice (Fig. 1C-C') and was detected in $41 \pm 8\%$ of all retinal Müller cells.

Gene expression of oxidative stress-related markers was altered in naïve MGCRe-FXN mice.

First, we evaluated whether FXN overexpression leads to changes in gene expression in naïve MGCRe-FXN mice. In the study we focused on markers well known to be involved in the retinal response and neuronal protection after lesion. These include neurotrophic factors such as leukemia inhibitory factor (*Lif*), nerve growth factor (*Ngf*), brain-derived neurotrophic factor (*Bdnf*), ciliary neurotrophic factor (*Cntf*) and glial cell line-derived neurotrophic factor (*Gdnf*), antioxidant enzymes including glutathione peroxidase 1 (*Gpx1*), superoxide dismutase [Cu-Zn] (*Sod1*), superoxide dismutase [Mn] (*Sod2*), catalase (*Cat*) and heme oxygenase 1 (*Hmox-1*), gliosis and inflammation markers including vimentin (*Vim*), glial fibrillary acidic protein (*Gfap*), glutamate aspartate transporter (*Glast*), glutamine synthetase (*Gs*), tumor necrosis factor alpha (*Tnf- α*) and Interleukin 1 beta (*Il-1 β*). We measured the relative mRNA expression by means of qRT-PCR and compared the values against those obtained in naïve non-transgenic MGCRe-B6 mice.

The expression levels of the growth factor *Bdnf* were significantly increased, whereas mRNA levels of *Cntf* and *Lif* were decreased in naïve MGCRe-FXN mice compared with control MGCRe-B6 mice (*Bdnf*: 1.22 ± 0.02 -fold increase, $P < 0.001$; *Cntf*: 0.83 ± 0.01 -fold decrease, $P < 0.001$; *Lif*: 0.41 ± 0.02 -fold decrease, $P < 0.05$, Fig. 2). The inflammation marker *Tnf- α* was significantly decreased in naïve transgenic retinae (0.55 ± 0.06 -fold decrease, $P < 0.05$, Fig. 2) and the antioxidative enzyme *Cat* was significantly increased (1.16 ± 0.07 -fold increase, $P < 0.05$, Fig. 2). Furthermore, the glia marker *Vim*, which is upregulated during gliosis, was decreased in naïve MGCRe-FXN mice (0.66 ± 0.05 vs. 1.00 ± 0.03 -fold decrease, $P < 0.05$, Fig. 2). The other markers tested did not differ in naïve MGCRe-FXN compared with MGCRe-B6 mice.

FXN overexpression in Müller cells increased RGC survival after ischemia/reperfusion. We next examined whether the expression of FXN in Müller cells increased survival of RGCs after acute ischemia/reperfusion. In naïve retinae from both, MGCRe-FXN and MGCRe-B6 mice, RGC distribution was highest around the optic nerve (1/6 from retinal radius) and decreased towards the periphery (5/6 from retinal radius). No differences in the overall cell distribution were observed between strains (Fig. 3A,B, Table 1).

After lesion, the number of RGCs decreased in MGCRe-B6 and MGCRe-FXN mice to $35 \pm 2\%$ ($P < 0.001$; $n = 6$) and $58 \pm 6\%$ ($P < 0.001$; $n = 8$) respectively, compared with non-lesioned control eyes (Fig. 3B'). This represents an increased RGC survival in mice overexpressing FXN of 65% 14 days after ischemia compared with MGCRe-B6 mice ($P < 0.05$, Fig. 3B').

Interestingly, as illustrated in Fig. 4A, the retinal thickness was increased in non-lesioned MGCRe-FXN mice compared with control animals. In particular, thickness of the GCL/IPL, as well as the INL, was increased by 24% and 13%, respectively. This was accompanied by a slight, but significant increase of basal IOP in naïve MGCRe-FXN mice (16 ± 0.3 mmHg vs. 14 ± 0.3 mmHg, $P < 0.05$, Fig. 4B).

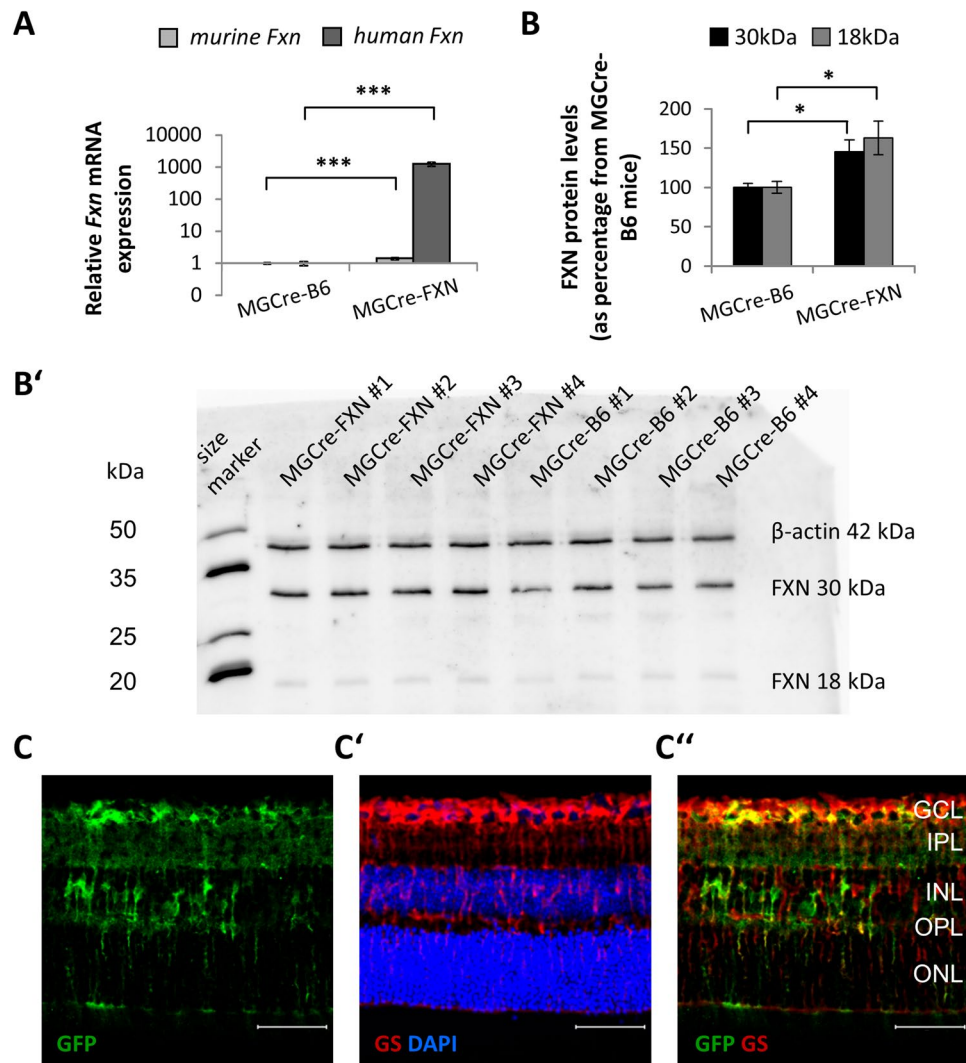


Figure 1. Expression of the human FXN transcript in the retina from MGCRe-FXN mice. **(A)** Relative expression of human FXN (*hFXN*) mRNA was determined by quantitative polymerase chain reaction, normalized against *Gapdh* and *Hprt* mRNA levels and depicted as fold increase of expression in MGCRe-B6 mice. The y-axis is depicted in logarithmic scaling. Bars represent the mean \pm SEM; $n = 6$; $***P < 0.001$. **(B)** FXN protein levels of precursor FXN form (30 kDa) and mature FXN form (18 kDa) were determined by densitometric analysis of Western blotting in MGCRe-B6 and MGCRe-FXN mice. Values are expressed as a percentage of MGCRe-B6 mice and normalized against β -actin. Bars represent the mean \pm SEM; $n = 4$; $*P < 0.05$. **(B')** Representative Western blot showing FXN precursor and mature bands for FXN in MGCRe-B6 and MGCRe-FXN mice. Full-length blot is presented in Supplementary Figure 1. **(C-C'')** GFP expression in MGCRe-FXN mice. Immunofluorescent staining of GFP (green), which is co-expressed with hFXN protein, and the Müller cell-specific marker glutamine synthetase (GS, red), as well as DAPI nuclear staining (blue) of retinal sections, were used to illustrate the hFXN location in Müller cells. GCL: ganglion cell layer, IPL: inner plexiform layer, INL: inner nuclear layer, OPL: outer plexiform layer, ONL: outer nuclear layer. Scale bar = $50\mu\text{m}$.

Retinal ischemia/reperfusion significantly reduced the thickness of the GCL/IPL by approximately 20% on average in MGCRe-FXN mice compared with MGCRe-B6 animals. Despite an increased neuronal survival, no differences in retinal thickness were found between strains after injury (Fig. 4A/C).

Increased expression of antioxidant enzymes in MGCRe-FXN mice after ischemia/reperfusion.

Gene expression ratios of the antioxidant enzymes *Gpx1*, *Sod1* and *Sod2*, *Cat* and *Hmox1* were evaluated 24 hours after ischemia by means of qRT-PCR to determine whether increased antioxidative capacity might be involved in FXN-mediated neuroprotection.

The expression levels of all enzymes evaluated were significantly increased in MGCRe-B6 mice after lesion compared to basal levels (*Gpx1*: 1.60 ± 0.05 -fold increase, $P < 0.001$; *Sod1*: 1.16 ± 0.03 -fold increase, $P < 0.001$; *Sod2*: 1.20 ± 0.02 -fold increase, $P < 0.001$; *Cat*: 1.31 ± 0.02 -fold increase, $P < 0.001$; *Hmox1*: 9.44 ± 0.72 -fold increase, $P < 0.001$).

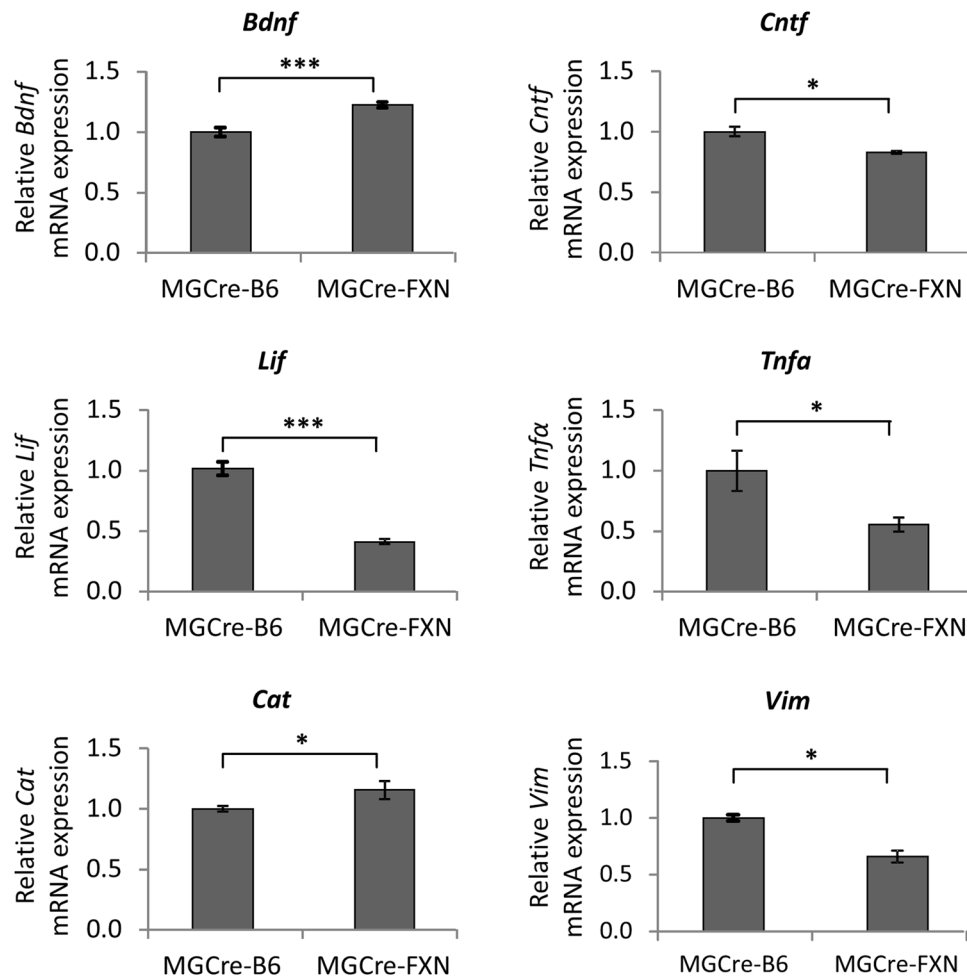


Figure 2. Effect of FXN overexpression on mRNA levels of the neurotrophic factors *Lif*, *Cntf* and *Bdnf*, tumor necrosis factor alpha (*Tnfa*), catalase (*Cat*) and vimentin (*Vim*) in the naïve mouse retina. Bars represent the mean \pm SEM, dashed lines represent 1.0 ratio, $n = 5$, * $P < 0.05$, *** $P < 0.001$, two-way ANOVA.

All tested markers also increased above basal levels in MGCRe-FXN mice after lesion, (*Gpx1*: 1.89 ± 0.05 -fold increase, $P < 0.001$; *Sod1*: 1.33 ± 0.06 -fold increase, $P < 0.001$; *Sod2*: 1.16 ± 0.05 -fold increase, $P < 0.001$; *Cat*: 1.33 ± 0.03 -fold increase, $P < 0.001$; *Hmox1*: 9.44 ± 1.56 -fold increase, $P < 0.001$). In addition, the expression levels of *Gpx1* and *Sod1* were significantly higher in MGCRe-FXN mice compared with the MGCRe-B6 animals after injury ($P < 0.05$; Fig. 5A).

Expression of neurotrophic factors is altered in MGCRe-FXN mice after lesion. To evaluate the role of growth factors in FXN-mediated neuroprotection, changes in expression of the growth factors *Gdnf*, *Ngf*, *Bdnf*, *Cntf* and *Lif* were analyzed 24 hours after ischemia by means of qRT-PCR.

The expression levels of *Ngf*, *Bdnf*, *Cntf* and *Lif* were significantly increased in MGCRe-B6 mice (*Ngf*: 1.60 ± 0.11 -fold increase, $P < 0.001$; *Bdnf*: 1.43 ± 0.03 -fold increase, $P < 0.001$; *Cntf*: 1.39 ± 0.09 -fold increase, $P < 0.001$; *Lif*: 8.44 ± 0.65 -fold increase, $P < 0.001$).

In MGCRe-FXN mice, all measured factors were also increased above basal levels 24 hours after ischemia (*Ngf*: 1.59 ± 0.16 -fold increase, $P < 0.001$; *Bdnf*: 1.36 ± 0.03 -fold increase, $P < 0.001$; *Cntf*: 1.8 ± 0.16 -fold increase, $P < 0.001$; *Lif*: 4.71 ± 1.06 -fold increase, $P < 0.001$).

Moreover, *Cntf* expression was higher and *Lif* expression was lower in MGCRe-FXN mice compared with MGCRe-B6 animals ($P < 0.05$; Fig. 5B).

Expression levels of inflammation and gliosis marker are not different between MGCRe-FXN and MGCRe-B6 mice after lesion. Expression of the cytokines *Tnf- α* and *Il-1 β* and of the gliosis marker *Glast*, *Vim*, *Gs* and *Gfap* were evaluated 24 hours after ischemia by means of qRT-PCR to determine whether inflammation or an altered gliotic response is involved in FXN-mediated neuroprotection.

Pro-inflammatory cytokines were significantly increased in MGCRe-B6 mice after lesion compared to basal levels (*Tnf- α* : 6.20 ± 0.42 -fold increase, $P < 0.001$; *Il-1 β* : 1.73 ± 0.21 -fold increase, $P < 0.001$). The expression levels of the intermediary filaments *Gfap* and *Vim* were increased after lesion, as well as the mRNA levels of *Glast*

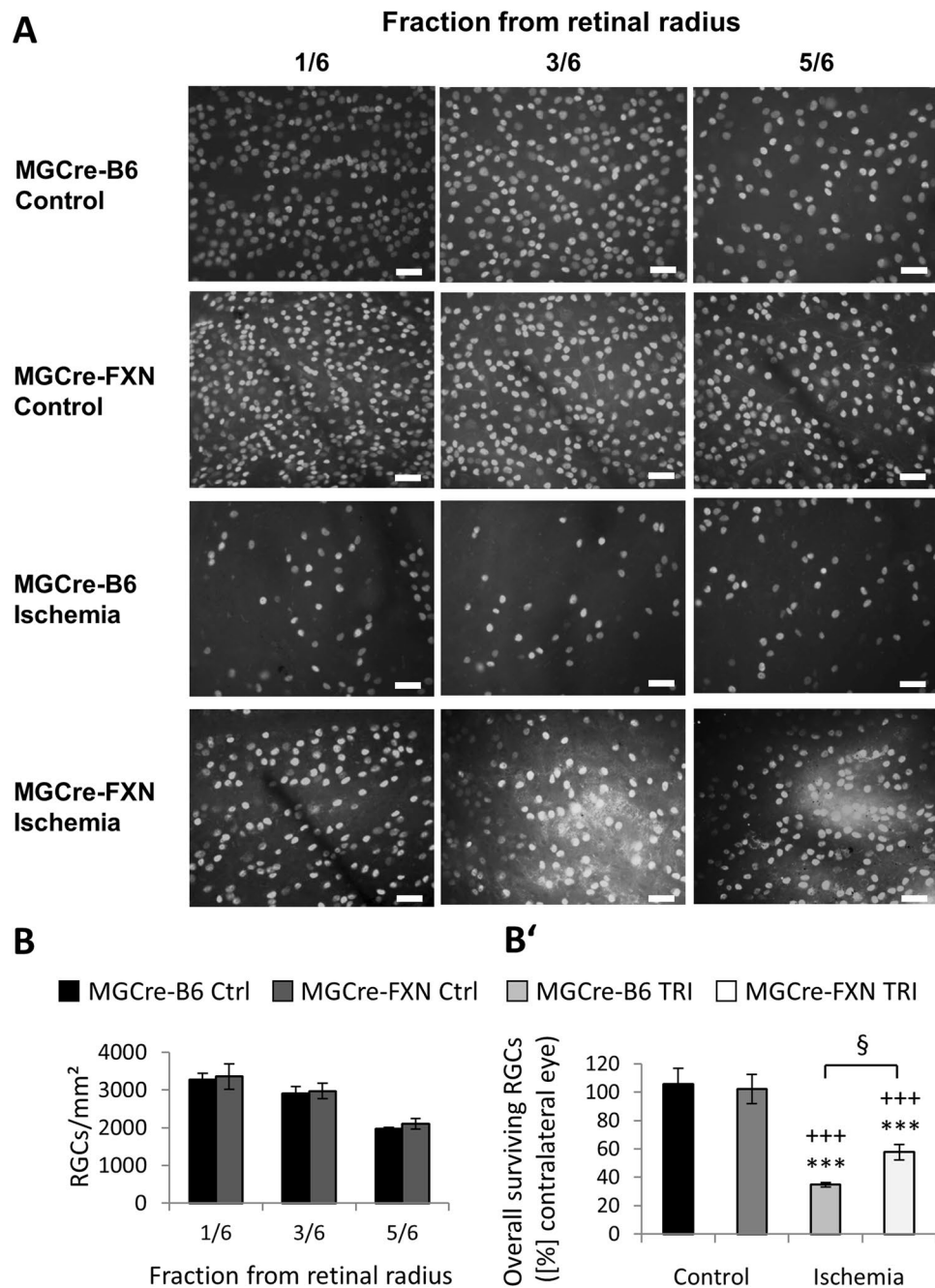


Figure 3. Effect of FXN overexpression in Müller cells on RGC survival 14 days after acute retinal ischemia/reperfusion. **(A)** Images of retinal whole-mount preparations from lesioned and non-lesioned MGCre-B6 and MGCre-FXN animals at various retinal eccentricities (1/6, 3/6, 5/6 from retinal radius) are shown. Images were taken with a fluorescence microscope (x40). Scale bars = 50 μ m. **(B)** Analysis of RGCs distribution per retinal eccentricity in non-lesioned MGCre-B6 and MGCre-FXN animals. Numbers of RGCs are expressed as cells/mm², n = 4. **(B')** Analysis of surviving RGCs after acute retinal ischemia/reperfusion. Numbers of RGCs are expressed as percentages from contralateral eyes. Cell counts were determined 14 days after the insult. Bars represent the mean \pm SEM; n = 4–8. $^{\$}P < 0.05$, $^{***}P < 0.001$ vs. MGCre-B6 Ctrl, $^{+++}P < 0.001$ vs. MGCre-FXN Ctrl.

(*Gfap*: 14.04 \pm 0.97-fold increase, $P < 0.001$; *Vim*: 5.47 \pm 0.31-fold increase, $P < 0.001$; *Glact*: 1.50 \pm 0.08-fold increase, $P < 0.001$). *Gs* levels decreased after ischemia (0.28 \pm 0.01-fold decrease, $P < 0.001$).

In MGCre-FXN mice, inflammatory markers were also increased above basal levels after lesion (*Tnf- α* : 6.82 \pm 0.97-fold increase, $P < 0.001$; *Il-1 β* : 1.62 \pm 0.48-fold increase, $P < 0.001$). Expression of the intermediary filaments *Gfap* and *Vim* as well as the levels of *Glact* were increased after injury (*Gfap*: 18.03 \pm 2.97-fold increase, $P < 0.001$; *Vim*: 4.63 \pm 0.53-fold increase, $P < 0.001$; *Glact*: 1.49 \pm 0.12-fold increase, $P < 0.001$). *Gs* levels decreased after ischemia (0.30 \pm 0.04-fold decrease, $P < 0.001$).

Treatment	Control			retinal ischemia/reperfusion		
retinal radius	1/6	3/6	5/6	1/6	3/6	5/6
mice strain	MGCre-B6					
RGC survival						
cells/mm ²	3275 ± 166	2912 ± 180	1975 ± 41	904 ± 99	891 ± 36	1063 ± 58
Percentage vs. contralateral eye	104 ± 11%	98 ± 13%	116 ± 9%	25 ± 3%	29 ± 1%	63 ± 5%
Mean ± SEM	106 ± 11%			35 ± 2%		
n=		4			6	
mice strain	MGCre-FXN					
RGC survival						
cells/mm ²	3258 ± 339	2974 ± 207	2103 ± 139	1358 ± 109*	1416 ± 159*	1098 ± 192
Percentage vs. contralateral eye	96 ± 10%	104 ± 11%	105 ± 12%	54 ± 9%*	54 ± 11%*	60 ± 9%
Mean ± SEM	102 ± 10%			58 ± 6%*		
n=	4			8		

Table 1. RGC quantification in murine retinal whole mount preparations as a function of the retinal radius.

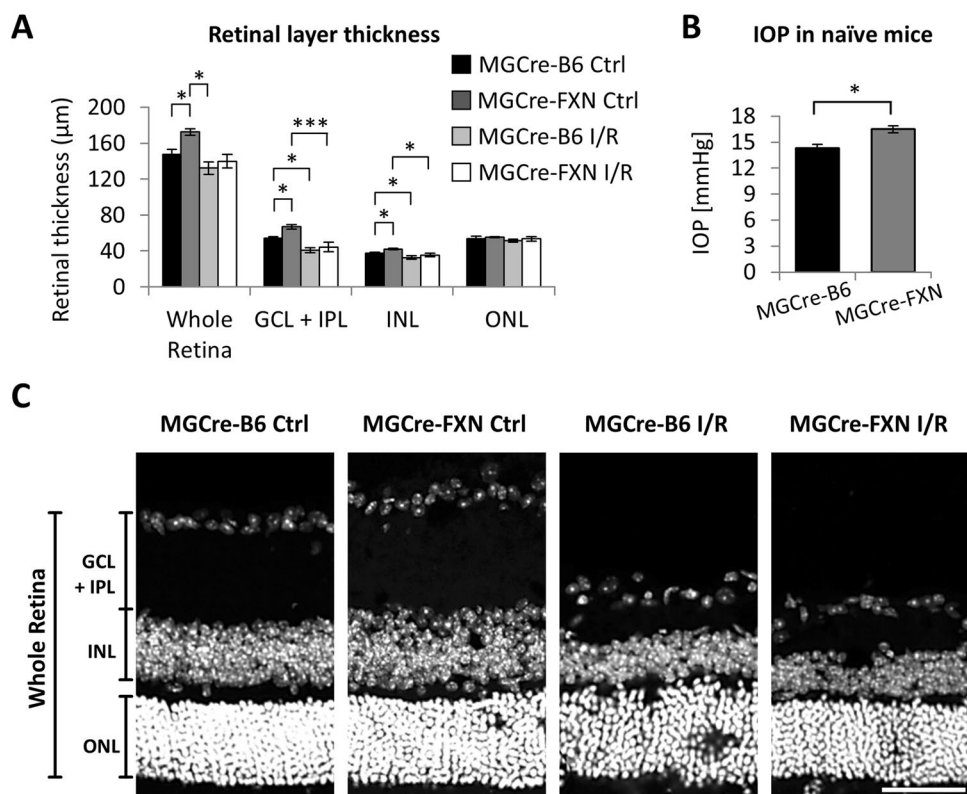


Figure 4. Effects of FXN overexpression on IOP and retinal morphology before and after acute ischemia/reperfusion. **(A)** Analysis of retinal layer thickness in naïve mice and after acute retinal ischemia/reperfusion. Ctrl: control, I/R: ischemia/reperfusion. Bars represent the mean ± SEM; n = 5. **P* < 0.05, ****P* < 0.001. **(B)** IOP measurement before increased IOP. Bars represent the mean ± SEM; MGCre-B6 n = 16, MGCre-FXN n = 50; **P* < 0.05, Mann-Whitney U Rank Sum Test. **(C)** Representative retinal sections through both control and ischemic retinæ from MGCre-B6 and MGCre-FXN mice are illustrated. Seven days after ischemia/reperfusion, retinal layers, particularly the IPL, are severely shrunk. GCL: ganglion cell layer, IPL: inner plexiform layer, INL: inner nuclear layer, OPL: outer plexiform layer, ONL: outer nuclear layer. Scale bar = 50 µm.

After ischemia, no differences in the expression of these markers were detected between MGCre-B6 background and MGCre-FXN transgenic mice.

Microglia response was impaired in MGCre-FXN mice after ischemia/reperfusion. Müller cells and microglia communicate via bidirectional signaling that can mediate adaptive responses within the retina following injury¹⁷. To determine whether FXN expression in Müller cells might influence the microglia response,

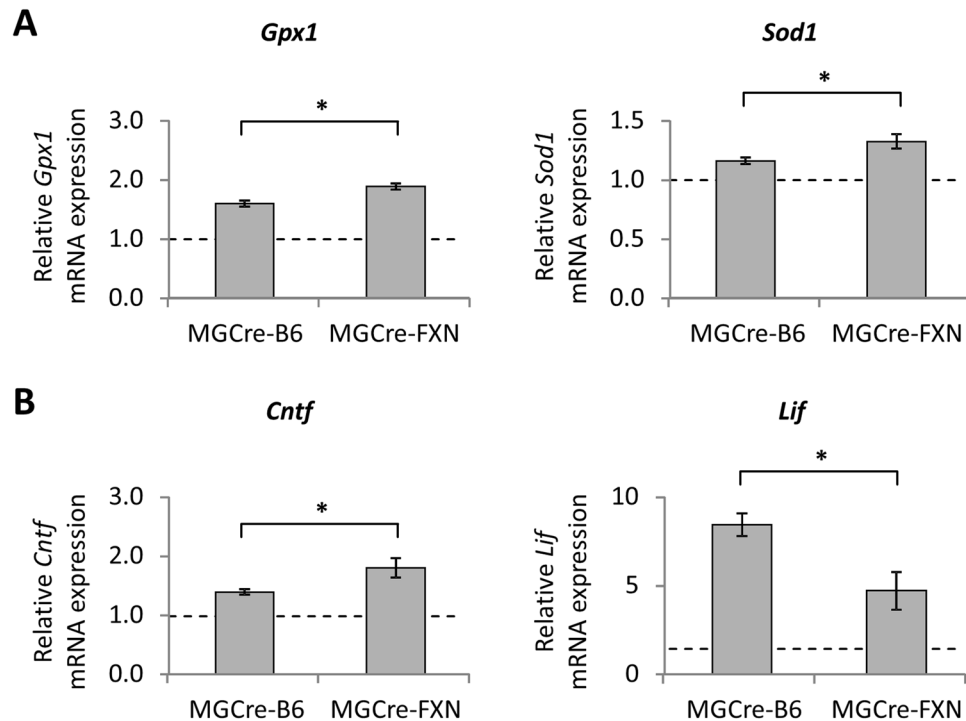


Figure 5. Effect of acute retinal ischemia/reperfusion and FXN overexpression on mRNA levels of (A) antioxidant enzymes *Gpx1* and *Sod1* and (B) neurotrophic factors *Cntf* and *Lif*. Expression levels of corresponding mRNAs were determined 24 hours after ischemia by quantitative polymerase chain reaction and normalized against *Gapdh* and *Hprt*. Bars represent the mean \pm SEM, dashed lines represent 1.0 ratio, $n = 5$, * $P < 0.05$, two-way ANOVA.

we evaluated the distribution of Iba1+ microglia and expression of the activation markers CD68 and MHCII in retinal slices before and after lesion. CD68 is a lysosomal protein and can be used to stain microglia in the retina. High expression levels are associated with reactive microglia, while low levels of expression are associated with quiescent ramified microglia^{18–20}. In addition, reactive microglia express the major histocompatibility complex class II (MHCII) for antigen presentation^{21,22}.

No differences in the number of Iba1+ microglia were observed in naïve retinæ of MGCRe-B6 and MGCRe-FXN mice (16 ± 2 and 14 ± 1 cells/1000 μm^2 , respectively, $P < 0.001$, Figs 6 and 7A). Few CD68 ($4.5 \pm 1\%$ and $8.3 \pm 1\%$, respectively) positive and almost no MHCII positive microglia were found ($2.8 \pm 1\%$ and $4.1 \pm 1\%$, respectively, Figs 6 and 7).

After ischemia, the percentage of Iba1+/Cd68+ microglia strongly increased in both, MGCRe-B6 and MGCRe-FXN mice; however, in MGCRe-FXN mice the number of CD68+ microglia was lower compared with MGCRe-B6 mice ($56 \pm 9\%$ vs. $81.1 \pm 1\%$; $P < 0.05$; Fig. 7B). The number of MHCII+ microglia after lesion increased only in MGCRe-B6 mice ($7.8 \pm 2\%$ vs. $2.8 \pm 1\%$; $P < 0.05$; Fig. 7C).

Discussion

In the present work, we generated a mouse model overexpressing human FXN specifically in retinal Müller cells. Naïve transgenic mice showed slightly decreased expression of gliosis and inflammation markers and of neurotrophic factors. After ischemia, we found an increased RGC survival in transgenic mice overexpressing FXN. Improved cell survival correlated with an increase in gene expression of antioxidant enzymes and neurotrophic factors, whereas the activity of retinal immune cells (microglia) was reduced.

In FXN overexpressing mice the expression levels of *hFXN* mRNA and FXN protein levels were significantly elevated in lysates from the whole retina. These data are similar to results obtained in a previous study using a transgenic mouse model with ubiquitous FXN in all retinal cells¹⁶. FXN overexpression was specifically increased in about 41% of all Müller cells. This value is similar to data shown in a previous study using the same Cre-recombinase expressing mice model²³. Naïve transgenic animals did not show differences in the number or distribution of RGCs and microglia as compared with MGCRe-B6 animals; however, morphological analysis of the naïve retina from FXN overexpressing mice showed an overall increase in retinal thickness, mainly manifested in the GCL and IPL but also in the INL. We also found a slight but significant increase in basal IOP levels in these animals. Different IOP levels ranging from 11.1 ± 0.5 mmHg to 19.3 ± 0.3 mmHg have been described in several different mouse strains, and have not been related to morphological changes or development of pathologies associated to elevated IOP including glaucoma²⁴.

Retinæ without Müller cells have decreased resistance to tensile stress rendering the retinal tissue to rip apart, a defect known as retinoschisis²⁵. Here, FXN overexpression seems to induce a similar effect by reducing the

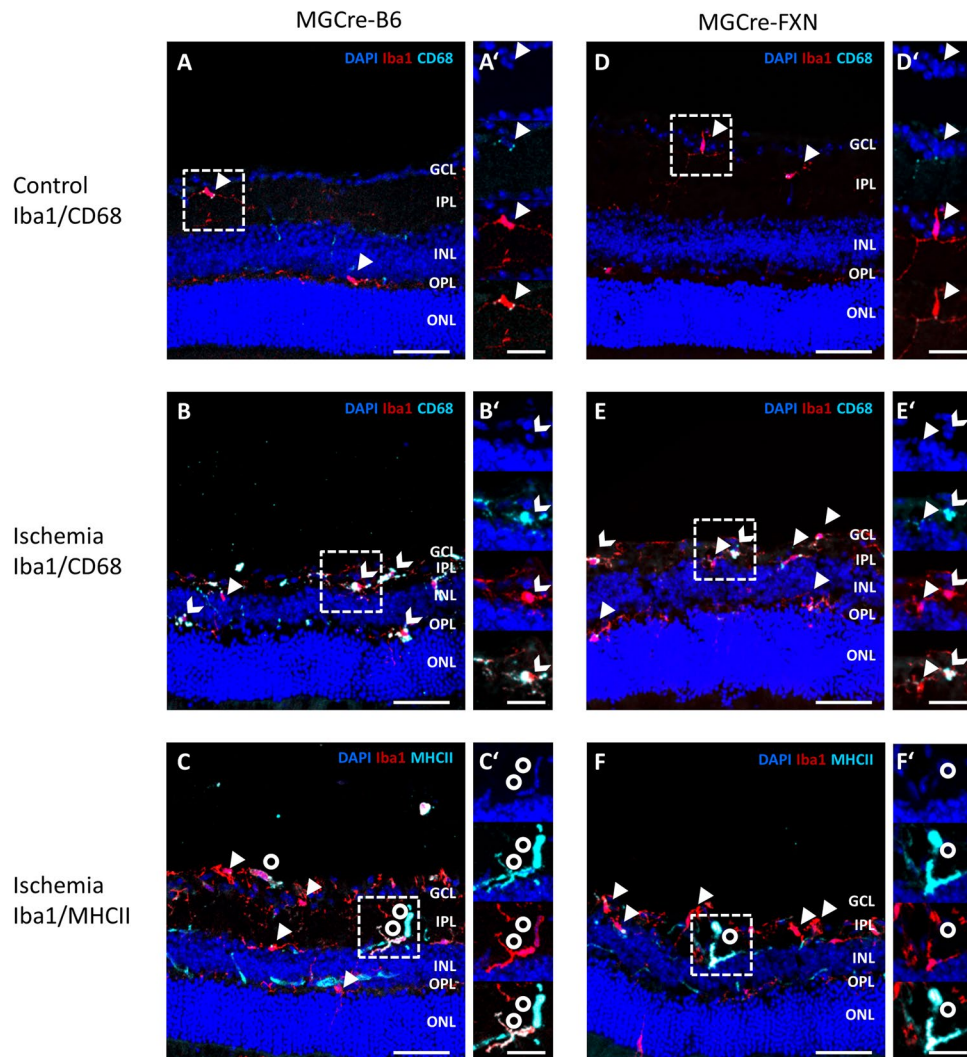


Figure 6. Distribution and localization of reactive microglia in the retina from MGCRe-B6 and MGCRe-FXN mice. Immunofluorescent staining for Iba1 (red), CD68 (cyan) or MHCII (cyan) as well as DAPI nuclear staining (blue) in retinal sections. Example sections of MGCRe-B6 (A–C) and MGCRe-FXN mice retinæ (D–F) before and after lesion are shown. Iba1+ microglia (arrowheads) and Iba1+ co-localized with CD68 (notched arrows) or MHCII (circles) were observed. GCL: ganglion cell layer, IPL: inner plexiform layer, INL: inner nuclear layer, OPL: outer plexiform layer, ONL: outer nuclear layer. Scale bar = 50 μm . (A'–C') and (D'–F') show enlarged squares containing example microglia with different merged channels for MGCRe-B6 and MGCRe-FXN mice. From top to bottom: DAPI; DAPI+ CD68 or MHCII; DAPI+ Iba1; Iba1+ CD68 or MHCII. Scale bar = 25 μm .

tensile strength of Müller cells, resulting in expanded retinal layers. The underlying mechanism is unknown, but could involve reduced levels of the intermediate filament vimentin and slight increased IOP levels found in these animals. Vimentin deficiency and mechanical stress have already been associated with a local separation of the inner limiting membrane leading to an increased retinal thickness²⁶. Furthermore, it was shown that undisturbed mice deficient for GFAP and vimentin (*GFAP^{-/-} vim^{-/-}*) display an altered Müller cell morphology and a decreased resistance to mechanical stress after induced retinal detachment²⁷.

There are only a few reports on transgenic mice strains overexpressing FXN and its associated effects. Mice expressing the full-length human FXN cDNA are normal with no signs of ataxia or other obvious abnormalities^{11,28}; however, these mice have an altered response during hematopoietic differentiation²⁸. The retina was not evaluated in that mouse model. For FXN overexpression, the existing literature presents contradictory results. On the one hand, experiments *in vivo* or *in vitro* in mice revealed that FXN overexpression was innocuous or had a positive effect on cell metabolism, stimulating the production of ATP or activating antioxidant mechanisms^{11,16,28–30}. In addition, overexpression of FXN in *Drosophila* promoted cellular resistance to oxidative stress⁸. On the other hand, FXN overexpression can lead to detrimental phenotypes in *Drosophila*, including developmental defects, a decrease in the level of aconitase activity, hypersensitivity to oxidative stress³¹, and reduced viability and impaired embryonic development of muscles and the peripheral nervous system³². Interestingly,

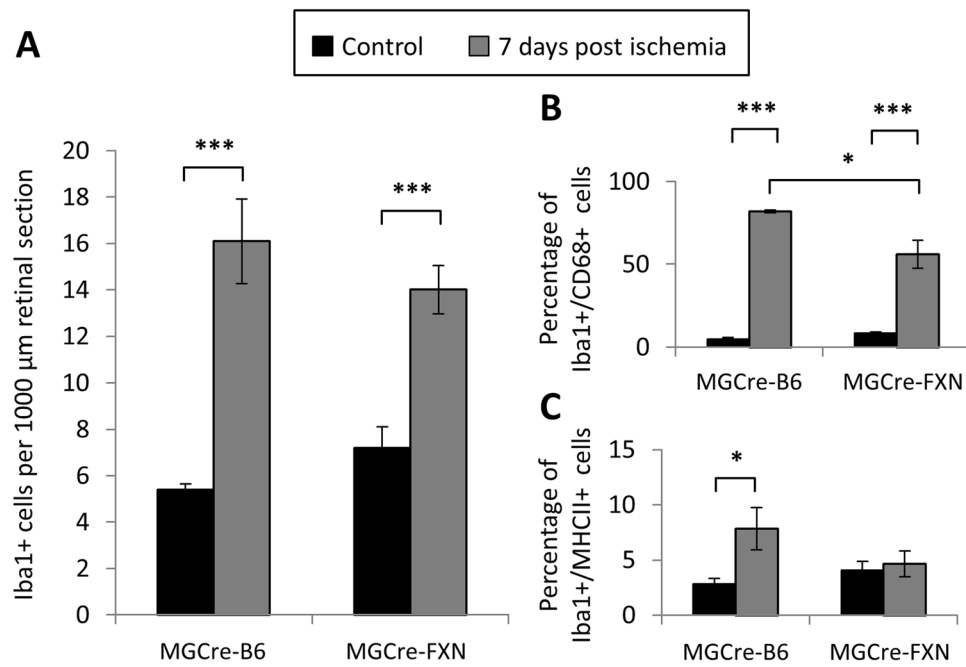


Figure 7. Effect of FXN on the expression of microglial reactivity markers. **(A)** Iba1+ cell counts per retinal section (1000 μm in length) in naïve and lesioned MGCRe-B6 and MGCRe-FXN mice. Bars represent the mean \pm SEM, $n = 5$, *** $P < 0.001$, two-way ANOVA. **(B)** Percentage of CD68 positive Iba1 cells in naïve and lesioned MGCRe-B6 and MGCRe-FXN mice. Bars represent the mean \pm SEM, $n = 5$, * $P < 0.05$, *** $P < 0.001$, two-way ANOVA. **(C)** Percentage of MHCII positive Iba1 cells in naïve and lesioned MGCRe-B6 and MGCRe-FXN mice. Bars represent the mean \pm SEM, $n = 5$, * $P < 0.05$, two-way ANOVA.

overexpression of FXN in yeast has also been shown to critically reduce aconitase activity, leading to impaired [Fe-S] cluster assembly and respiration³³. The mechanisms responsible for these effects are not known, but FXN aggregation and a misfolding of the protein have been shown not to be the cause for the phenotypes that have been observed³². Importantly, also in yeast, frataxin overproduction increased cellular antioxidant defenses³³. In our study, FXN overexpression in Müller cells led to changes in the basal gene expression of several factors. Increased *Cat* might improve retinal homeostasis by providing a less oxidative environment, as also suggested by decreased *Lif* expression²⁸. BDNF levels are known to be associated with increased expression of antioxidant proteins and reduced oxidative stress levels^{34,35}. Therefore, increased *Bdnf* levels in naïve FXN overexpressing mice might also be indicative of decreased ROS levels, even before lesion onset.

Retinal ischemia/reperfusion injury leads to a high loss of RGCs in MGCRe-B6 mice, comparable to values obtained in a previous study from our lab using C57BL/6J mice¹⁶. Here, we show for the first time that specific FXN overexpression in Müller cells leads to a significant increase in neuronal survival after lesion. Interestingly, we achieved the same level of neuroprotection compared to transgenic mice with ubiquitous FXN overexpression in the retina¹⁶. This strongly indicates that Müller cells play a critical role in FXN-mediated neuroprotection after the ischemic lesion.

One of the hallmarks of acute retinal ischemia/reperfusion is the generation of excessive ROS leading to neuronal cell death. Müller cells are well known to protect neuronal cells from oxidative stress by providing antioxidants such as glutathione³⁶. Since protective effects mediated by FXN overexpression are known to also involve several antioxidant mechanisms^{28,30}, we tested the effect of increased FXN expression on levels of antioxidant enzymes, including *Gpx1*, *Sod1*, *Sod2*, *Cat*, and *Hmox1*. The expression of all enzymes was increased in the retinae of both MGCRe-B6 and MGCRe-FXN mice after ischemia, in agreement with other studies^{2,37,38}. Importantly, *Gpx1* and *Sod1* were higher expressed in transgenic mice than in MGCRe-B6 mice. Both factors are already described to be neuroprotective^{39,40}. These results are also in agreement with our previous study involving FXN overexpression in the retina, where we found increased levels of *Gpx1*, *Sod1*, *Sod2* and *Cat* transcripts after lesion¹⁶. This supports our previous findings showing that FXN mediates neuroprotection after ischemia by promoting the antioxidant response. To evaluate further mechanisms involved in neuroprotection by FXN expression in Müller cells, we measured the expression levels of growth factors, including *Bdnf*, *Gdnf*, *Ngf*, *Lif* and *Cntf*. Neurotrophic factors are known to have neuroprotective properties⁴¹ and have been suggested to be part of an endogenous response mechanism after an ischemic insult⁴². In agreement with other studies, we found an increase in *Bdnf*, *Ngf*, *Lif* and *Cntf* levels following ischemia-reperfusion in both MGCRe-B6 and FXN overexpressing mice⁴³⁻⁴⁷. Interestingly, in our study, only *Cntf* increased significantly over nontransgenic levels after lesion. CNTF has been described to be neuroprotective for photoreceptor cells⁴⁸⁻⁵⁰ and RGCs in several studies⁵¹⁻⁵⁴. In the retina, CNTF is expressed by various cell types and particularly by Müller cells⁵⁵. Increased *Cntf* transcripts strongly support an important role of Müller cells in FXN-mediated neuroprotection. In contrast, *Lif*

transcripts did not reach the expression level of nontransgenic animals after lesion. However, it was significantly increased above transgenic basal levels. LIF is an important endogenous neuroprotective factor in the retina^{56,57}. Specifically, photoreceptor injuries induce a subset of Müller cells to express LIF⁵⁶. Further, its transcript seems to be stabilized by H₂O₂⁵⁸. Together with the increased antioxidative response, these results indicate that FXN potentiates Müller cell-mediated neuroprotection after acute retinal ischemia/reperfusion by increasing the neurotrophic support.

Our results show a decreased microglia response after transient ischemia in transgenic mice overexpressing FXN in Müller cells. In models of RGC damage, the extent of microgliosis negatively correlates with the number of surviving RGCs⁵⁹. A decreased number of microglia would be expected with increased neuronal survival; however, we did not observe differences in microglial numbers after lesion in nontransgenic and transgenic mice. Interestingly, the number of reactive microglia, as indicated by the expression of CD68 and MHCII, was decreased in FXN overexpressing mice after ischemia. CD68 and MHCII are markers of microglia activation reflecting phagocytic and immune activity, respectively^{19–22,60,61}. Microglia reactivity and inflammation are common hallmarks of a broad spectrum of retinal diseases and contribute to RGC loss associated with ON damage in glaucoma⁶² and retinal ischemia⁶³. Blocking microglia reactivity is known to be neuroprotective e.g. in experimental glaucoma^{64–66}. Our results are in agreement with studies showing that the expression of MHCII is upregulated in activated microglia during axonal degeneration induced by ocular hypertension in rats^{67,68} and downregulated MHCII is associated with less severe axonal degeneration in a model of glaucoma by chronic increased IOP⁶⁸. Reduced expression levels of MHCII may inhibit the activation of invading T-cell, thereby diminishing the inflammatory cascade leading to tissue damage^{69,70}. Decreased CD68 positive microglia might reflect a reduced phagocytic activity associated with an increased neuronal survival in MGCe-FXN mice after lesion. The phagocytic activity of microglia is associated to clearance of cells debris, and of damaged or dying cells⁶¹. On the other hand, Müller cells and microglia actively cross-talk to maintain constant levels of neurotrophic factors important for retinal physiology^{71,72}. Microglia can directly trigger the release of several neurotrophic factors from Müller cells, including GDNF, LIF, CNTF and NGF^{17,56,73,74}. Furthermore, vimentin expression serves as a marker for activated states of microglia^{18,19,75}. In our study, FXN-overexpressing Müller cells seemed to regulate microglial function under physiological conditions, as suggested by reduced vimentin expression in naïve retinae. We propose that FXN-mediated modulation of the Müller cell response to lesion impacts microglial reactivity, possibly by reducing the number of cells in the reactive M1-state, as seen by unchanged expression of MHCII and decreased number of CD68 positive cells in MGCe-FXN mice following injury^{61,76}.

Taken together, our results show that FXN overexpression in Müller cells improves RGC survival after acute ischemia/reperfusion injury and this is associated with an increased expression of antioxidant enzymes and neurotrophic factors. Furthermore, our study highlights Müller cells as important players in retinal pathologies and indicates that support of the glial management of retinal redox homeostasis might constitute a therapeutic alternative to overcome neuronal degeneration due to increased oxidative stress.

Materials and Methods

Animal Guidelines. All experiments were performed in accordance with the European Convention for Animal Care and with the ARVO Statement for the Use of Animals in Ophthalmic and Vision Research and were also approved by the local animal care committee (Thüringer Landesamt für Verbraucherschutz (TLV) - Abteilung 2 Gesundheitlicher und technischer Verbraucherschutz, accreditation numbers: 02-047/08 and 02-013/11). Animals were housed in standard cages in groups of 5 animals on a 14-hour light/10-hour dark cycle, with food and water available *ad libitum*, a temperature ranging from 22 °C to 25 °C and humidity ranging from 55% to 60%.

Male C57BL/6J background and transgenic mice overexpressing FXN, weighing 25 ± 2 g, aged 12 ± 1 weeks, were used in the study. Transgenic animals overexpressing FXN in Müller cells were generated by breeding homozygous mice carrying cassettes of human PVMD2-rtTA and TRE-cre (PVMD2TREcre^{23,77,78}, provided by Dr. Yun-Zheng Le, Department of Cell Biology, University of Oklahoma Health Sciences Center, Oklahoma City, USA) to heterozygous mice carrying a CMV-driven human FXN cDNA preceded by a loxP-flanked stop cassette (R26CMVFXN/wt, provided by Prof. Michael Ristow, Department of Health Sciences and Technology, Swiss Federal Institute of Technology, Zürich, Switzerland), hereafter referred to as MGCe-FXN. Cre-mediated excision of the stop cassette leads to expression of the FXN gene and of green fluorescent protein (EGFP), as has been shown in our previous work with ubiquitous FXN overexpressing mice¹⁶. Background mice were generated by breeding C57BL/6J with PVMD2TREcre mice, hereafter referred to as MGCe-B6. Mice were randomized for each experimental setup into a non-lesioned group (MGCe-B6 n = 22; MGCe-FXN n = 22) or an ischemia group (MGCe-B6 n = 16; MGCe-FXN n = 18).

Retinal ischemia/reperfusion injury. Retinal ischemia/reperfusion injury was performed as previously described^{16,79}. Briefly, mice were anesthetized with an intraperitoneal injection of 5% chloral hydrate in phosphate buffered saline (PBS; 500 mg/kg body weight; Fluka, Seelze, Germany). After application of topical anesthesia (4 mg/ml oxybuprocaine-hydrochloride; Bausch & Lomb GmbH, Feldkirchen, Germany), the anterior chamber of the right eye was cannulated with a 30-gauge needle connected to an elevated normal saline reservoir. Intraocular pressure (IOP) was elevated above systolic pressure (increased from 15.5 ± 2.6 mmHg to 93 ± 4.4 mmHg) for 45 minutes. IOP was measured using an induction/impact tonometer (TonoLab; Tiolat Ltd., Helsinki, Finland). This method has been validated for the mouse eye⁸⁰. One drop of antibiotic solution (ofloxacin; Bausch & Lomb GmbH, Berlin, Germany) was applied topically to the treated eye after cannulation. After 45 minutes of ischemia, the needle was withdrawn and the IOP normalized. Treated eyes were inspected daily and animals with signs of inflammation or iatrogenic cataract were excluded from the study. Animals for RGC evaluation were sacrificed with an overdose of chloral hydrate (30%) 14 days after ischemia, as previously described¹⁶.

For microglia analysis, mice were sacrificed 7 days after lesion, coinciding with highest microglial proliferation as already reported⁵⁹. For qRT-PCR analysis, mice were sacrificed 24 hours post ischemia as described in a previous study¹⁶.

Retinal tissue fixation and sectioning. To localize human FXN (hFXN) expression and evaluate microglia response after ischemic injury, retinal sections from background and MGCRe-FXN mice were prepared. Briefly, animals were sacrificed with an overdose of chloral hydrate (30%), eyes were removed and fixed in 4% PFA for 20 min at room temperature (RT), enucleated, again fixed in 4% PFA for 20 min, washed in PBS and cryoprotected by immersion in 30% sucrose in PBS overnight at 4 °C. Eyecups were then frozen in an appropriate embedding medium (Tissue Tek; Sakura, Loeterwoude, The Netherlands) and cryosectioned into 16 µm slices.

Retinal whole mounts of MGCRe-B6 and MGCRe-FXN mice were prepared to evaluate RGC survival following ischemia. Eyes were enucleated and retinæ were removed and fixed by immersion in 4% PFA for 20 min. After washing in PBS, retinæ were flattened by making incisions from the periphery halfway to the optic nerve to form four symmetric lobes.

Immunofluorescent staining. Immunofluorescent staining protocols were similar for retinal slices and whole mounts. Retinal sections were dried at 37 °C for 45 min and fixed with 4% PFA for 20 min. Retinal whole mounts were permeabilized with 0.3% Triton X-100 in PBS for 45 min at RT. Blocking was achieved by incubation with 3% bovine serum albumin (BSA) and 10% normal donkey serum (NDS) in PBS supplemented with 0.3% Triton X-100 for 2 hours at RT. After non-specific binding was blocked, whole mounts were incubated with primary antibody raised against the RGC-specific transcription factor Brn3a (goat anti-Brn3a, 1:300; Santa Cruz, Heidelberg, Germany), whereas slices were incubated with primary antibodies directed against ionized calcium-binding adaptor molecule (rabbit anti-Iba1, 1:500; Wako, Neuss, Germany), cluster of differentiation 68 (rat anti-CD68, 1:200; Serotec, Düsseldorf, Germany), major histocompatibility complex class II (rat anti-MHCII, 1:10,000; affymetrix, CA, USA), GFP (goat anti-GFP, 1:100, Acris, Herford, Germany) and glutamine synthetase (mouse anti-GS, 1:250, Millipore, Darmstadt, Germany) in 5% NDS, overnight at 4 °C. After washing with PBS, probes were incubated with corresponding secondary antibodies (Molecular Probes, Leiden, The Netherlands) in 10% NDS for one hour at RT. For nucleic acid staining, the retinal slices were immersed into a DAPI (4'-6-Diamidino-2-phenylindole) solution for 5 min. Specificity of the staining was tested by incubation without primary antibody.

Fluorescence microscopy. RGC survival was evaluated on retinal whole mounts 14 days post-ischemia. Brn3a-labeled RGCs were counted in single fields at three different retinal eccentricities in each of the four whole mount lobes (1/6, 3/6 and 5/6 from retinal radius; 0.093 mm² each, 12 fields in total) according to Schmeer *et al.*⁸¹ and Schultz *et al.*¹⁶. The number of surviving RGCs was expressed as the number of cells per square millimeter and cell counts were given as the percentage of corresponding contralateral and non-lesioned eyes.

The number of GFP+ Müller cells specifically expressing FXN was determined on slices from MGCRe-FXN mice by counting GS+ GFP+ cell processes located in the IPL. The results are given as percentage from the whole GS+ cell population.

The number of Iba1+ microglia was determined on retinal sections. Cell counts were corrected for slice length and expressed as cell count per 1000 µm. The number of reactive microglia was assessed by counting Iba1+ CD68+ and Iba1+MHCII+ cells.

Image acquisition and cell counting was performed by fluorescence microscopy (40x magnification, Axioplan2 Imaging microscope; Carl Zeiss Meditec, Jena, Germany) on retinal whole mounts and by confocal laser scanning microscopy using the ZEN software (40× magnification, 710 Meta; Carl Zeiss Meditec) on retinal slices. Experimenters were blinded for animal genotype and treatment.

Quantitative polymerase chain reaction analysis. Eyes were enucleated 24 hours post ischemia and retinæ were shock frozen in liquid nitrogen. Isolation of mRNA was carried out using standard protocols with the QIAzol lysis reagent (Qiagen, Hilden, Germany). RNA concentration and purity were determined by spectrophotometry (NanoDrop 2000c; Peqlab/VWR, Darmstadt, HE, Germany). DNA contamination and RNA integrity, as assessed by the RNA Integrity Score, were determined using the QIAxcel RNA QC Kit v2.0 (Qiagen) with the QIAxcel Advanced system (Qiagen). Equal amounts of total retinal mRNA (100 ng/µl) were reversely transcribed into cDNA using a Revert Aid First Strand cDNA Synthesis Kit (Thermo Scientific, Schwerte, Germany). Real-time qPCR was carried out with Brilliant II SYBR Green QPCR Mastermix (Agilent Technologies, Santa Clara, CA, USA). A final cDNA concentration of 25 ng per 20 µl of sample volume including 500 nM specific primers was used. After denaturing at 95 °C for 10 min, 40 amplification cycles were carried out as follows: denaturation at 95 °C for 60 s, annealing at 60 °C for 30 s, and elongation at 72 °C for 30 s.

Primer sequences were selected/designed to exclusively recognize specific target sequences using the Primer-BLAST online tool⁸². The primer specificity and predicted target size were confirmed by capillary electrophoresis. The primer sequences for murine (*mFxn*) and human FXN (*hFXN*), antioxidant enzymes, neurotrophic factors and inflammatory cytokines are depicted in Table 2. Glyceraldehyde 3-phosphate dehydrogenase (*Gapdh*) and hypoxanthine-guanine phosphoribosyltransferase (*Hprt*) were used as housekeeping genes. Relative expression ratios (fold changes) of the target genes were calculated using the Pfaffl method⁸³.

Western blotting. To evaluate the protein levels of retinal FXN in MGCRe-B6 and MGCRe-FXN mice, Western blotting was performed as previously described¹⁶. Primary antibodies raised against FXN (1:500; Santa Cruz), β-Actin (1:10,000; abcam, Cambridge, UK) and horseradish peroxidase (HRP)-conjugated secondary antibody (1:5000 dilution) were used. Protein bands were visualized using an enhanced chemiluminescence reaction kit (Immun-Star WesternC Chemiluminescence Kit, BioRad, München, Germany), photographed with Fujifilm

Gene name		Primer Seq. (5' -> 3')	Prod. size (bp)
hFXN	Fw	CCTTGCAGACAAGCCATACA	150
human Fratxin	Rev	CCACTGGATGGAGAAGATAG	
Fxn	Fw	CCTGGCCGAGTTCTTTGAAG	152
mouse FXN	Rev	GCCAGATTTGCTTGTTTGG	
Antioxidant response			
Gpx1	Fw	GGGACTACACCGAGATGAACGA	197
glutathione peroxidase 1	Rev	ACCATTCACTTCGCACTTCTCA	
Sod1	Fw	GTCCGTCGGCTTCTCGTCT	163
superoxide dismutase [Cu-Zn]	Rev	CACAACCTGGTTCACCGCTTG	
Sod2	Fw	ATTAACGCGCAGATCATGCA	161
superoxide dismutase [Mn]	Rev	TGTCCCCACCATTGAACTT	
Cat	Fw	GCAGATACCTGTGAACTGTC	229
catalase	Rev	GTAGAATGTCCGCACCTGAG	
Hmox1	Fw	GGTGATGGCTTCCTTGACC	155
heme oxygenase 1	Rev	AGTGAGGCCCATACCAGAAG	
Glial response			
Vim	Fw	TGAAGGAAGAGATGGCTCGT	194
Vimentin	Rev	GGTGTCAACCAGAGGAAGTGA	
Gfap	Fw	AGAAAGGTTGAATCGCTGGA	176
glial fibrillary acidic protein	Rev	GCCACTGCCTCGTATTGAGT	
Glast	Fw	GCCCTCCGACCGTATAAAAT	128
Glutamate aspartate transporter	Rev	GCCATTCTGTGACGAGACT	
Gs	Fw	ATCGGGTGTGCGAAGACTTT	181
glutamine synthetase	Rev	CGAATGTGGTACTGGTGCCT	
Neurotrophic factors			
Lif	Fw	AATGCCACCTGTGCCATACG	216
leukemia inhibitory factor	Rev	CAACTTGGTCTTCTCTGTCCCG	
Ngf	Fw	AGCATTCCCTTGACACAG	99
nerve growth factor	Rev	GGTCTACAGTGATGTTGC	
Bdnf	Fw	TGGCTGACACTTTTGACCAC	131
brain-derived neurotrophic factor	Rev	CAAAGGCACTTGACTGCTGA	
Cntf	Fw	ATGACTGAGGCAGAGCGACT	157
ciliary neurotrophic factor	Rev	AGGCAGAACTTGGAGCGTA	
Gdnf	Fw	TGGGCTATGAAACCAAGGAG	142
glial cell line-derived neurotrophic factor	Rev	CAACATGCCTGGCCTACTTT	
Inflammatory markers			
Tnf-alpha	Fw	GTCTACTGAACTTCGGGGTGAT	102
Tumor necrosis factor alpha	Rev	ATGATCTGAGTGTGAGGGTCTG	
Il1b	Fw	GAAGAGCCCATCCTCTGTGA	96
Interleukin 1 beta	Rev	TTCATCTCGGAGCCTGTAGTG	
Housekeeping genes			
Hprt	Fw	TGACACTGGTAAACAATGCA	94
hypoxanthine-guanine phosphoribosyltransferase	Rev	GGTCCTTTTACCAGCAAGCT	
Gapdh	Fw	AGGTCGGGTGAACGGATTTG	123
Glyceraldehyde 3-phosphate dehydrogenase	Rev	TGTAGACCATGTAGTTGAGGTCA	

Table 2. Primer sequences for mRNAs analyzed in the study, together with the expected product length. fw, forward primer; rev, reverse primer.

LAS-3000 Imager and analyzed with ImageJ software (1.46v). Measurements were done in duplicate. Each band was normalized against the corresponding β -actin band. Changes in protein expression were expressed as a percentage of control mice.

Statistical Analysis. All results are expressed as the mean \pm standard error of the mean (SEM). Each group consisted of at least four animals. Proof of normal distribution was done for all data by a Shapiro-Wilk test. For RGC survival analysis, statistical significance was assessed by using one-way ANOVA followed by Holm-Sidak post hoc analysis and comparing MGCRe-B6 control mice and treatment groups. For relative gene expression analysis, ratio data were log₂ transformed and two-way ANOVA followed by Holm-Sidak post hoc analysis was

applied for comparison of lesion effects between mice strains. For microglia cell counts and reactivity marker expression, two-way ANOVA followed by Holm-Sidak post hoc analysis was applied for comparison of lesion effects between mice strains. For Western blot analysis, the results were compared by one-way ANOVA followed by Holm-Sidak post hoc analysis comparing background and transgenic mice. SigmaPlot (13.0v) was used and the level of significance was set at $P < 0.05$.

Data availability. The datasets generated during and/or analyzed during the current study are available from the corresponding author on reasonable request.

References

- Inman, D., Lupien, C. & Horner, P. Manipulating glia to protect retinal ganglion cells in glaucoma. *Cdn. Intechweb. Org* <https://doi.org/10.5772/20441> (2001).
- Arai-Gaun, S. *et al.* Heme Oxygenase-1 Induced in Müller Cells Plays a Protective Role in Retinal Ischemia–Reperfusion Injury in Rats. *Investig. Ophthalmol. Vis. Sci.* **45**, 4226–32 (2004).
- Vázquez-Chona, F. R. *et al.* Proliferative reactive gliosis is compatible with glial metabolic support and neuronal function. *BMC Neurosci.* **12**, 98 (2011).
- Wurm, A. *et al.* Effects of ischemia-reperfusion on physiological properties of Müller glial cells in the porcine retina. *Investig. Ophthalmol. Vis. Sci.* **52**, 3360–3367 (2011).
- Frantseva, M. V., Carlen, P. L. & Perez Velazquez, J. L. Dynamics of intracellular calcium and free radical production during ischemia in pyramidal neurons. *Free Radic. Biol. Med.* **31**, 1216–1227 (2001).
- Osborne, N. N. *et al.* Retinal ischemia: Mechanisms of damage and potential therapeutic strategies. *Prog. Retin. Eye Res.* **23**, 91–147 (2004).
- Kim, M. J. *et al.* Protective effects of transduced PEP-1-Frataxin protein on oxidative stress-induced neuronal cell death. *J. Neurol. Sci.* **298**, 64–69 (2010).
- Runko, A. P., Griswold, A. J. & Min, K. T. Overexpression of frataxin in the mitochondria increases resistance to oxidative stress and extends lifespan in *Drosophila*. *FEBS Lett.* **582**, 715–719 (2008).
- Schulz, J. B. *et al.* Oxidative stress in patients with Friedreich ataxia. *Neurology* **55**, 1719–1721 (2000).
- Ristow, M. *et al.* Frataxin activates mitochondrial energy conversion and oxidative phosphorylation. *Proc. Natl. Acad. Sci. USA* **97**, 12239–43 (2000).
- Schulz, T. J. *et al.* Activation of mitochondrial energy metabolism protects against cardiac failure. *Aging (Albany, NY)*. **2**, 843–853 (2010).
- Koutnikova, H. *et al.* Studies of human, mouse and yeast homologues indicate a mitochondrial function for frataxin. *Nat. Genet.* **16**, 345–351 (1997).
- Efimova, M. G. & Trotter, Y. Distribution of frataxin in eye retina of normal mice and of transgenic R7E mice with retinal degeneration. *J. Evol. Biochem. Physiol.* **46**, 414–417 (2010).
- Aartsen, W. M. *et al.* GFAP-driven GFP expression in activated mouse Müller glial cells aligning retinal blood vessels following intravitreal injection of AAV2/6 vectors. *PLoS One* **5** (2010).
- Bringmann, A. *et al.* Cellular signaling and factors involved in Müller cell gliosis: Neuroprotective and detrimental effects. *Prog. Retin. Eye Res.* **28**, 423–451 (2009).
- Schultz, R., Witte, O. W. & Schmeer, C. Increased frataxin levels protect retinal ganglion cells after acute ischemia/reperfusion in the mouse retina *in vivo*. *Investig. Ophthalmol. Vis. Sci.* **57**, 4115–4124 (2016).
- Wang, M., Ma, W., Zhao, L., Fariss, R. N. & Wong, W. T. Adaptive Müller cell responses to microglial activation mediate neuroprotection and coordinate inflammation in the retina. *J. Neuroinflammation* **8**, 173 (2011).
- Graeber, M. B., Streit, W. J. & Kreutzberg, G. W. The microglial cytoskeleton: vimentin is localized within activated cells *in situ*. *J. Neurocytol.* **17**, 573–580 (1988).
- Slepko, N. & Levi, G. Progressive activation of adult microglial cells *in vitro*. *Glia* **16**, 241–246 (1996).
- Kingham, P. J., Cuzner, M. L. & Pocock, J. M. Apoptotic pathways mobilized in microglia and neurones as a consequence of chromogranin A-induced microglial activation. *J. Neurochem.* **73**, 538–547 (1999).
- Streit, W. J., Walter, S. A. & Pennell, N. A. Reactive microgliosis. *Prog. Neurobiol.* **57**, 563–581 (1999).
- Benveniste, E. N., Nguyen, V. T. & O’Keefe, G. M. Immunological aspects of microglia: Relevance to Alzheimer’s disease. *Neurochem. Int.* **39**, 381–391 (2001).
- Ueki, Y., Ash, J. D., Zhu, M., Zheng, L. & Le, Y. Z. Expression of Cre recombinase in retinal Muller cells. *Vision Res.* **49**, 615–621 (2009).
- Savinova, O. V. *et al.* Intraocular pressure in genetically distinct mice: an update and strain survey. *BMC Genet* **2**, 12 (2001).
- MacDonald, R. B. *et al.* Müller glia provide essential tensile strength to the developing retina. *J. Cell Biol.* **210**, 1075–1083 (2015).
- Lundkvist, A. *et al.* Under stress, the absence of intermediate filaments from Muller cells in the retina has structural and functional consequences. *J. Cell Sci* **117**, 3481–3488 (2004).
- Verardo, M. R. *et al.* Abnormal reactivity of Müller cells after retinal detachment in mice deficient in GFAP and vimentin. *Investig. Ophthalmol. Vis. Sci.* **49**, 3659–3665 (2008).
- Miranda, C. J. *et al.* Frataxin overexpressing mice. *FEBS Lett.* **572**, 281–288 (2004).
- Shoichet, S. A. *et al.* Frataxin promotes antioxidant defense in a thiol-dependent manner resulting in diminished malignant transformation *in vitro*. *Hum. Mol. Genet.* **11**, 815–821 (2002).
- Schulz, T. J. *et al.* Induction of oxidative metabolism by mitochondrial frataxin inhibits cancer growth: Otto Warburg revisited. *J. Biol. Chem.* **281**, 977–981 (2006).
- Llorens, J. V. *et al.* Causative role of oxidative stress in a *Drosophila* model of Friedreich ataxia. *FASEB J.* **21**, 333–344 (2007).
- Navarro, J. A. *et al.* Overexpression of human and fly frataxins in *drosophila* provokes deleterious effects at biochemical, physiological and developmental levels. *PLoS One* **6** (2011).
- Seguin, A. *et al.* Overexpression of the yeast frataxin homolog (Yfh1): Contrasting effects on iron-sulfur cluster assembly, heme synthesis and resistance to oxidative stress. *Mitochondrion* **9**, 130–138 (2009).
- Sasaki, M. *et al.* Neurodegenerative influence of oxidative stress in the retina of a murine model of diabetes. *Diabetologia* **53**, 971–979 (2010).
- Gardiner, J., Barton, D., Overall, R. & Marc, J. Neurotrophic support and oxidative stress: converging effects in the normal and diseased nervous system. *Neuroscientist* **15**, 47–61 (2009).
- Schütte, M. & Werner, P. Redistribution of glutathione in the ischemic rat retina. *Neurosci. Lett.* **246**, 53–56 (1998).
- Andreeva, K. *et al.* Time-dependent Gene Profiling Indicates the Presence of Different Phases for Ischemia/Reperfusion Injury in Retina. *Ophthalmol. Eye Dis.* **6**, 43–54 (2014).
- Agardh, C. D., Gustavsson, C., Hagert, P., Nilsson, M. & Agardh, E. Expression of antioxidant enzymes in rat retinal ischemia followed by reperfusion. *Metabolism.* **55**, 892–898 (2006).

39. Ishibashi, N., Prokopenko, O., Weisbrot-Lefkowitz, M., Reuhl, K. R. & Mirochnitchenko, O. Glutathione peroxidase inhibits cell death and glial activation following experimental stroke. *Mol. Brain Res.* **109**, 34–44 (2002).
40. Yuki, K., Yoshida, T., Miyake, S., Tsubota, K. & Ozawa, Y. Neuroprotective role of superoxide dismutase 1 in retinal ganglion cells and inner nuclear layer cells against N-methyl-D-aspartate-induced cytotoxicity. *Exp. Eye Res.* **115**, 230–8 (2013).
41. Kimura, A., Namekata, K., Guo, X., Harada, C. & Harada, T. Neuroprotection, growth factors and BDNF-TRKB signalling in retinal degeneration. *Int. J. Mol. Sci.* **17** (2016).
42. Bringmann, A. & Wiedemann, P. Müller glial cells in retinal disease. *Ophthalmologica* **227**, 1–19 (2011).
43. Lönnngren, U. *et al.* The growth factor response in ischemic rat retina and superior colliculus after brimonidine pre-treatment. *Brain Res. Bull.* **71**, 208–218 (2006).
44. Miyazaki, H., Nagashima, K., Okuma, Y. & Nomura, Y. Expression of glial cell line-derived neurotrophic factor induced by transient forebrain ischemia in rats. *Brain Res.* **922**, 165–172 (2001).
45. Yang, X. C. & Duan, X. C. Minocycline inhibits the production of the precursor form of nerve growth factor by retinal microglial cells. *Neural Regen. Res.* **8**, 320–327 (2013).
46. Sanchez, R. N. *et al.* Interleukin-6 in retinal ischemia reperfusion injury in rats. *Investig. Ophthalmol. Vis. Sci.* **44**, 4006–4011 (2003).
47. Gustavsson, C., Agardh, C.-D., Hagert, P. & Agardh, E. Inflammatory markers in nondiabetic and diabetic rat retinas exposed to ischemia followed by reperfusion. *Retina* **28**, 645–652 (2008).
48. Cayouette, M., Behn, D., Sendtner, M., Lachapelle, P. & Gravel, C. Intraocular gene transfer of ciliary neurotrophic factor prevents death and increases responsiveness of rod photoreceptors in the retinal degeneration slow mouse. *J. Neurosci.* **18**, 9282–93 (1998).
49. Chong, N. H. V. *et al.* Repeated injections of a ciliary neurotrophic factor analogue leading to long-term photoreceptor survival in hereditary retinal degeneration. *Investig. Ophthalmol. Vis. Sci.* **40**, 1298–1305 (1999).
50. Rhee, K. D. *et al.* CNTF-mediated protection of photoreceptors requires initial activation of the cytokine receptor gp130 in Müller glial cells. *Proc. Natl. Acad. Sci.* **110**, E4520–E4529 (2013).
51. Mey, J. & Thanos, S. Intravitreal injections of neurotrophic factors support the survival of axotomized retinal ganglion cells in adult rats *in vivo*. *Brain Res.* **602**, 304–317 (1993).
52. Maier, K. *et al.* Ciliary neurotrophic factor protects retinal ganglion cells from secondary cell death during acute autoimmune optic neuritis in rats. *Brain Pathol.* **14**, 378–87 (2004).
53. Pease, M. E. *et al.* Effect of CNTF on retinal ganglion cell survival in experimental glaucoma. *Investig. Ophthalmol. Vis. Sci.* **50**, 2194–200 (2009).
54. Mathews, M. K., Guo, Y., Langenberg, P. & Bernstein, S. L. Ciliary neurotrophic factor (CNTF)-mediated ganglion cell survival in a rodent model of non-arteritic anterior ischaemic optic neuropathy (NAION). *Br. J. Ophthalmol.* **99**, 133–137 (2015).
55. Kirsch, M., Lee, M. Y., Meyer, V., Wiese, A. & Hofmann, H. D. Evidence for multiple, local functions of ciliary neurotrophic factor (CNTF) in retinal development: expression of CNTF and its receptors and *in vitro* effects on target cells. *J. Neurochem.* **68**, 979–990 (1997).
56. Joly, S., Lange, C., Thiersch, M., Samardzija, M. & Grimm, C. Leukemia Inhibitory Factor Extends the Lifespan of Injured Photoreceptors *In Vivo*. *J. Neurosci.* **28**, 13765–13774 (2008).
57. Leibinger, M. *et al.* Neuroprotective and axon growth-promoting effects following inflammatory stimulation on mature retinal ganglion cells in mice depend on ciliary neurotrophic factor and leukemia inhibitory factor. *J. Neurosci.* **29**, 14334 LP–14341 (2009).
58. Agca, C. *et al.* Expression of leukemia inhibitory factor in Müller glia cells is regulated by a redox-dependent mRNA stability mechanism. *BMC Biol.* **13**, 30 (2015).
59. Liu, S. *et al.* Tracking retinal microgliosis in models of retinal ganglion cell damage. *Investig. Ophthalmol. Vis. Sci.* **53**, 6254–6262 (2012).
60. Graeber, M. B., Streit, W. J., Kiefer, R., Schoen, S. W. & Kreutzberg, G. W. New expression of myelomonocytic antigens by microglia and perivascular cells following lethal motor neuron injury. *J. Neuroimmunol.* **27**, 121–132 (1990).
61. Perego, C., Fumagalli, S. & De Simoni, M. G. Temporal pattern of expression and colocalization of microglia/macrophage phenotype markers following brain ischemic injury in mice. *J. Neuroinflammation* **8** (2011).
62. Yuan, L. & Neufeld, A. H. Activated microglia in the human glaucomatous optic nerve head. *J. Neurosci. Res.* **64**, 523–532 (2001).
63. Naskar, R., Wissing, M. & Thanos, S. Detection of early neuron degeneration and accompanying microglial responses in the retina of a rat model of glaucoma. *Investig. Ophthalmol. Vis. Sci.* **43**, 2962–2968 (2002).
64. Ai, L. W. *et al.* Minocycline inhibits LPS-induced retinal microglia activation. *Neurochem. Int.* **47**, 152–158 (2005).
65. Levkovitch-Verbin, H., Kalev-Landoy, M., Habot-Wilner, Z. & Melamed, S. Minocycline delays death of retinal ganglion cells in experimental glaucoma and after optic nerve transection. *Arch. Ophthalmol.* **124**, 520–526 (2006).
66. Levkovitch-Verbin, H., Waserzoog, Y., Vander, S., Makarovsky, D. & Piven, I. Minocycline upregulates pro-survival genes and downregulates pro-apoptotic genes in experimental glaucoma. *Graefes Arch. Clin. Exp. Ophthalmol.* **52**, 761–772 (2014).
67. Ebnetter, A., Casson, R. J., Wood, J. P. M. & Chidlow, G. Microglial activation in the visual pathway in experimental glaucoma: Spatiotemporal characterization and correlation with axonal injury. *Investig. Ophthalmol. Vis. Sci.* **51**, 6448–6460 (2010).
68. Chidlow, G., Ebnetter, A., Wood, J. P. M. & Casson, R. J. Evidence supporting an association between expression of major histocompatibility complex II by microglia and optic nerve degeneration during experimental glaucoma. *J. Glaucoma* **25**, 681–691 (2016).
69. Tezel, G. *et al.* The role of glia, mitochondria, and the immune system in glaucoma. In *Investigative Ophthalmology and Visual Science* **50**, 1001–1012 (2009).
70. Shao, H., Kaplan, H. J. & Sun, D. Major histocompatibility complex molecules on parenchymal cells of the target organ protect against autoimmune disease. *Chem. Immunol. Allergy* **92**, 94–104 (2007).
71. Harada, T. *et al.* Microglia–Müller glia cell interactions control neurotrophic factor production during light-induced retinal degeneration. *J. Neurosci.* **22**, 9228 LP–9236 (2002).
72. Wang, M. *et al.* Macrogliia–microglia interactions via TSPO signaling regulates microglial activation in the mouse retina. *J. Neurosci.* **34**, 3793–806 (2014).
73. Carwile, M. E., Culbert, R. B., Sturdivant, R. L. & Kraft, T. W. Rod outer segment maintenance is enhanced in the presence of bFGF, CNTF and GDNF. *Exp. Eye Res.* **66**, 791–805 (1998).
74. Harada, C. *et al.* Potential role of glial cell line-derived neurotrophic factor receptors in Müller glial cells during light-induced retinal degeneration. *Neuroscience* **122**, 229–235 (2003).
75. Jiang, S. X., Slinn, J., Aylsworth, A. & Hou, S. T. Vimentin participates in microglia activation and neurotoxicity in cerebral ischemia. *J. Neurochem.* **122**, 764–774 (2012).
76. Cherry, J. D., Olschowka, J. A. & O'Banion, M. Neuroinflammation and M2 microglia: the good, the bad, and the inflamed. *J. Neuroinflammation* **11**, 98 (2014).
77. Zhu, M., Zheng, L., Ueki, Y., Ash, J. D. & Le, Y. Z. Unexpected transcriptional activity of the human VMD2 promoter in retinal development. In *Advances in Experimental Medicine and Biology* **664**, 211–216 (2010).
78. Le, Y. Z. *et al.* Inducible expression of Cre recombinase in the retinal pigmented epithelium. *Investig. Ophthalmol. Vis. Sci.* **49**, 1248–1253 (2008).
79. Krempler, K., Schmeer, C. W., Isenmann, S., Witte, O. W. & Löwel, S. Simvastatin improves retinal ganglion cell survival and spatial vision after acute retinal ischemia/reperfusion in mice. *Investig. Ophthalmol. Vis. Sci.* **52**, 2606–2618 (2011).

80. Daniais, J., Kontiola, A. I., Filippopoulos, T. & Mittag, T. Method for the noninvasive measurement of intraocular pressure in mice. *Investig. Ophthalmol. Vis. Sci.* **44**, 1138–1141 (2003).
81. Schmeer, C., Gámez, A., Tausch, S., Witte, O. W. & Isenmann, S. Statins modulate heat shock protein expression and enhance retinal ganglion cell survival after transient retinal ischemia/reperfusion *in vivo*. *Investig. Ophthalmol. Vis. Sci.* **49**, 4971–4981 (2008).
82. Ye, J. *et al.* Primer-BLAST: A tool to design target-specific primers for polymerase chain reaction. *BMC Bioinformatics* **13**, 134 (2012).
83. Pfaffl, M. W. A new mathematical model for relative quantification in real-time RT-PCR. *Nucleic Acids Res.* **29**, e45 (2001).

Acknowledgements

This work was supported by a grant from the Deutsche Forschungsgemeinschaft (DFG) (SCHM2639/1-1) to C.S. OWW received support from the Bundesministerium für Bildung und Forschung (BMBF) Bernstein Fokus (01GQ0923). BMBF Gerontosys/JenAge (031 5581B), DFG FOR 1738 WI 830/10-2, DFG Schwerpunktprogramm BU 1327/4-1.

Author Contributions

The Contribution of each author are as follows: study design (C.S.), experimental work (R.S.), data acquisition (R.S., M.K., M.P., S.G.W.), data analysis (R.S.), manuscript discussion (O.W.W.), manuscript preparation (R.S., C.S.). All authors reviewed the manuscript.

Additional Information

Supplementary information accompanies this paper at <https://doi.org/10.1038/s41598-018-22887-5>.

Competing Interests: The authors declare no competing interests.

Publisher's note: Springer Nature remains neutral with regard to jurisdictional claims in published maps and institutional affiliations.



Open Access This article is licensed under a Creative Commons Attribution 4.0 International License, which permits use, sharing, adaptation, distribution and reproduction in any medium or format, as long as you give appropriate credit to the original author(s) and the source, provide a link to the Creative Commons license, and indicate if changes were made. The images or other third party material in this article are included in the article's Creative Commons license, unless indicated otherwise in a credit line to the material. If material is not included in the article's Creative Commons license and your intended use is not permitted by statutory regulation or exceeds the permitted use, you will need to obtain permission directly from the copyright holder. To view a copy of this license, visit <http://creativecommons.org/licenses/by/4.0/>.

© The Author(s) 2018